MODELLING OF AIRCREW RADIATION EXPOSURE FROM SOLAR PARTICLE EVENTS

H. AL ANID, B.J. LEWIS, AND L.G.I. BENNETT

Department of Chemistry and Chemical Engineering, Royal Military College of Canada, P.O. Box 17000, Stn Forces, Kingston, Ontario, K7K 7B4, Canada

Abstract

A transport code analysis using the Monte Carlo code, MCNPX, has been used to propagate an extrapolated particle spectrum based on GOES satellite measurements through the atmosphere to estimate aircrew radiation exposure due to solar particle events. Neutron monitor count rate data from ground stations around the world were used to benchmark the model calculations during several Ground Level Events (GLEs). In addition, a comparison was made between the model predictions and actual flight measurements made by some European investigators with various types of instruments used to measure the mixed radiation field during GLE 60 and 65. A computer-code has been further developed to implement the model for routine analysis.

1. Introduction

In 1990, the International Commission on Radiological Protection (ICRP) recognized the occupational exposure of aircrew to cosmic radiation. [1] In Canada, a Commercial and Business Aviation Advisory Circular (CBAAC) was issued by Transport Canada suggesting that action should be taken to manage such exposure. [2] In anticipation of possible regulations on exposure of Canadian-based aircrew in the near future, an extensive study was carried out at RMC by the Nuclear Research Group to estimate the radiation absorbed during flights.

The radiation exposure to aircrew is a result of a complex mixed-radiation field resulting from *Galactic Cosmic Rays* (GCRs) and *Solar Energetic Particles* (SEPs). Supernova explosions and active galactic nuclei are responsible for GCRs which consist of 90% protons, 9% alpha particles, and 1% heavy nuclei. [3] While they have a fairly constant fluence rate, their interaction with the solar magnetic field of the Earth varies throughout the solar cycles, which has a period of approximately 11 years. The radiation dose absorbed on airplanes due to GCR has been thoroughly studied and the empirical-based PC-AIRE code developed at RMC can predict the radiation dose with good accuracy.

SEPs are highly sporadic events that are associated with solar flares and coronal mass ejections. While contributing less than 1% to the overall career exposure, this type of exposure may be of concern to certain aircrew members, such as pregnant flight crew, where the annual effective dose is limited to 1 mSv over the remainder of the pregnancy. [4] The composition of SEPs is very similar to GCRs, in that they consist of mostly protons, some alpha particles and a few heavy nuclei, but with a different energy spectrum.

To estimate the additional exposure due to solar flares, a model was developed using a transport code analysis with MCNPX; a Monte-Carlo radiation transport code. The model transports an extrapolated flux spectrum through the atmosphere using the MCNPX analysis. This code produces the estimated flux at a specific altitude where ICRP conversion rates are applied to convert the particle flux into an ambient dose equivalent. Transporting the flux through the atmosphere to ground level enables calculations of expected neutron-monitor count rates, which can be compared against NM data obtained from stations all around the world.

2. Model Development

2.1 Solar Flare Particle Spectrum

The particle spectrum resulting from a solar flare is highly variable and sporadic. Satellite measurements provide near real-time data; one specific instrument is the Space Environment Monitor (SEM) on the Geostationary Operational Environmental Satellites (GOES). The SEM is capable of measuring the flux of solar and galactic particles and X-rays. The proton flux measurements necessary for our model are provided by energetic particle sensors (EPS) and the high-energy proton and alpha detector (HEPAD), which operate over a large range of energies (Table 1).

In order to transport the particle spectrum through the atmosphere the GOES measurements must be extrapolated to a high energy of 10 GeV, which is accomplished by fitting the GOES data to a power-law equation for the differential flux using:

$$\phi(E) = \frac{C}{\beta}\left(\frac{R}{R_o}\right)^{-\gamma} \quad \textbf{(1)}$$

The particle rigidity R (in MV) is related to its energy E (in MeV) by the relation:

$$R = \sqrt{E(E + 2E_o)} \quad \textbf{(2)}$$

where $E_o = m_o c^2$ is the rest mass energy of the particle (in MeV) and $\beta = R/\,(R^2 + E_o^2)^{1/2}$ is the particle velocity v normalized by the speed of light c. The parameter R_o = 239 MV in **(1)** corresponds to a particle energy of E = 30 MeV.

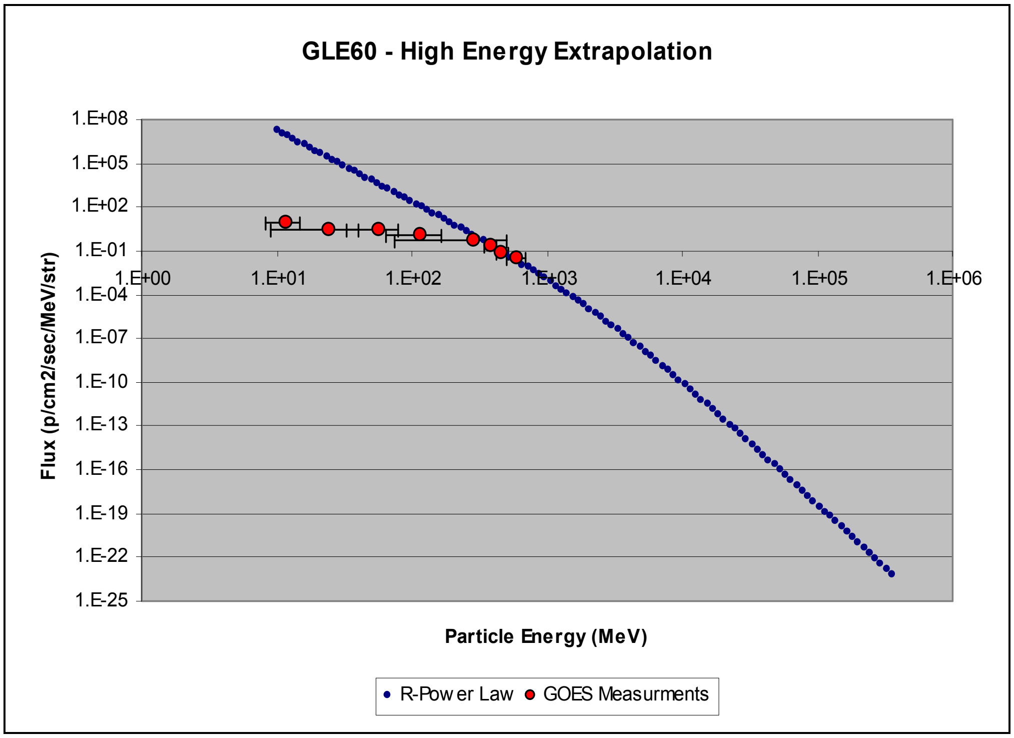

Figure 1 – High-Energy extrapolation of differential proton energy data from the GOES satellite for GLE 60.

2.2 MCNPX Analysis

The MCNPX code (version 2.5) was used to determine the particle production and transport in the atmosphere. Although secondary particles are produced by interaction of primary cosmic ray particles with atmospheric nuclei, only the production of neutrons and protons were considered. The atmosphere was divided into 36 concentric shells using an average air density for a given shell thickness. Secondary particle energy spectra produced from an incident mono-energetic source particle was tracked in the analysis. [5] Combined particle spectra (at a given altitude) were therefore obtained by summing the secondary particle spectra derived from each mono-energetic primary particle based on the initial proton spectrum and helium spectrum. Dose conversion factors as well as neutron monitor response functions have been incorporated with the MCNPX results for a specific altitude. [6]

As a preliminary test, the interstellar GCR spectrum was used to predict neutron and proton spectra on the ground and at 17 km. These results were compared to those measured by Goldhagen and Gordon and were determined to be in reasonable agreement. [7-9] Based on this agreement, the MCNPX analysis was applied to the SEP particle spectrum. For the GCR spectrum, a spherical geometry was used, since galactic rays are assumed to be isotropic, arriving from any direction. For the solar flare code, planer source geometry was used. Figure 2 illustrates both geometries for transporting particles through the Earth's atmosphere.

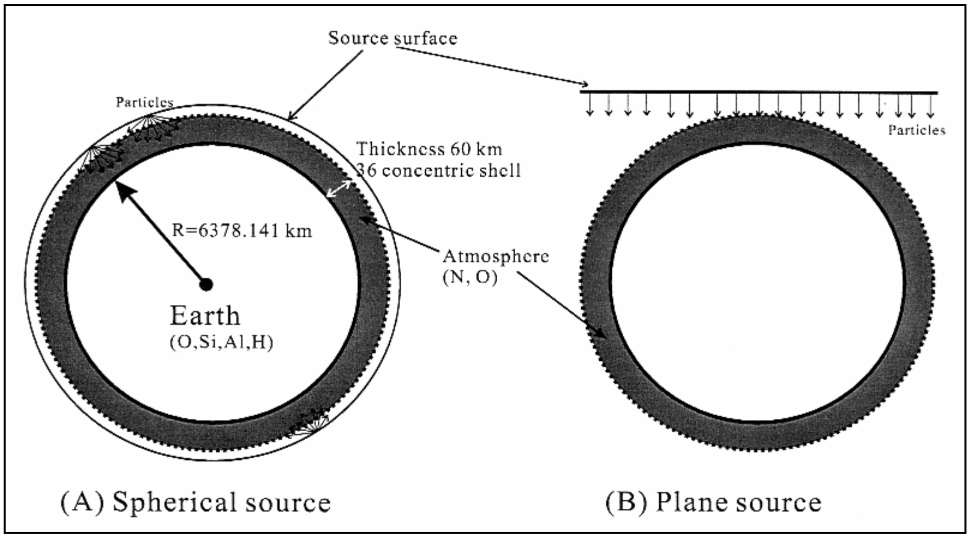

Figure 2 – Spherical and Planer geometry for MCNPX transport code

2.3 Vertical Cut-off Rigidity

The Earth's magnetic field acts as a shield to incoming particles and radiation. Particles that do not have sufficient energy to penetrate the Earth's field bounce off the magnetic shield back into space. Therefore, a model of the cutoff rigidity has to take into account the properties of the Earth's magnetic field as well as geographical position.

During an SPE, the Earth is bombarded with energetic particles causing major disturbances in the field. Not only do the particles contribute largely to the already-existing radiation (due to GCR), the solar wind during a geomagnetic storm can squish the Earth's magnetic field thus lowering the cutoff rigidity.

The effect of the cutoff rigidity is taken into consideration in the calculation by summing up only those particles with energies greater than the vertical cutoff rigidity R_c. A low pass energy filter was applied to match the NM data where primary protons with energy less than 430 MeV were ignored in the summation. This filter was chosen by matching predicted results to observed ground-level NM data (See Table 2 for NM characteristics). This filter accounts for the attenuation of the lower-energy particles from the GOES satellite to the top layer of the atmosphere, as well as possible anisotropic effects of the solar flare as it reaches the Earth. Figure 3 illustrates the prediction of the model using various cutoff filters, leading to the final choice of 1 GV. Figure 4 show a comparison between the predicted NM count rates against data from NM stations around the world for GLE 60.

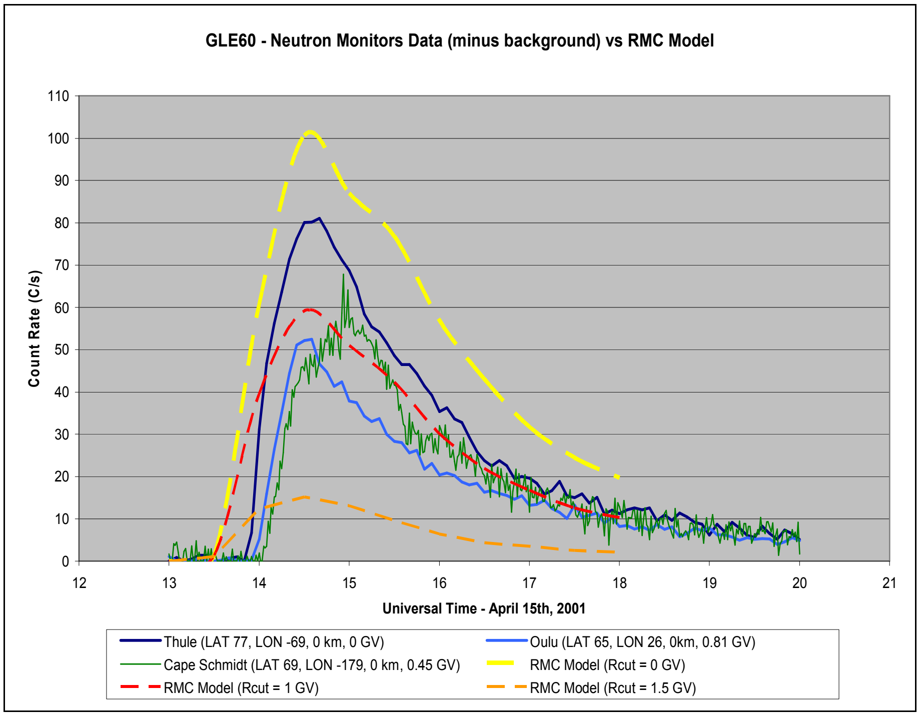

Figure 3 – Observed count rate history (minus GCR background) versus model predictions for GLE 60.

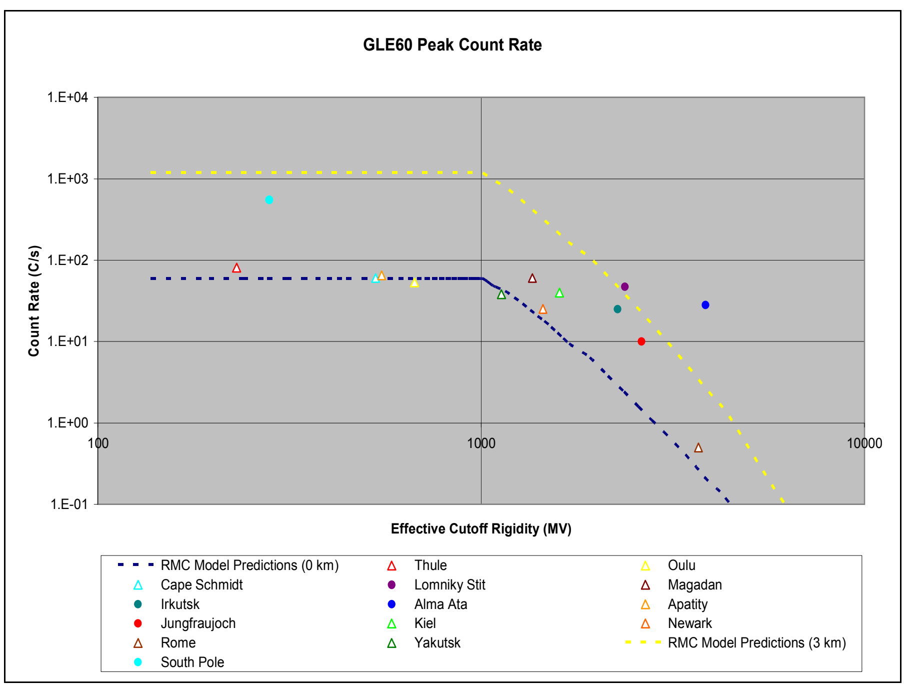

Figure 4 – Comparison of the model calculations to the observed peak count rates for various NMs located around the world during GLE 60. (Circles represent NMs at an altitude of 3 km, triangles represent NMs at an altitude of 0 km)

3.0 Results and Analysis

To test the validity of the model, it was necessary to perform the solar flare calculation on GLEs where actual flight measurements exist, allowing direct comparison. One such event is GLE 60, where flight measurements were taken as part of the DOSMAX project. The results are illustrated in Figures 5a and 5b. As seen in Figure 5 (a), for example, the solar flare contributed 45% to the total cumulative dose of 54 μSv for the PRG-JFK route.

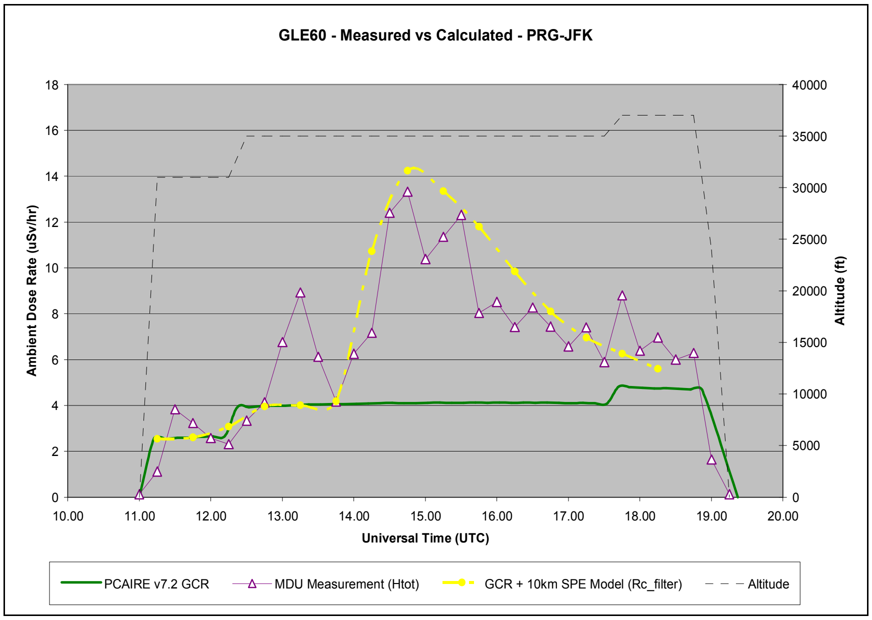

(a)

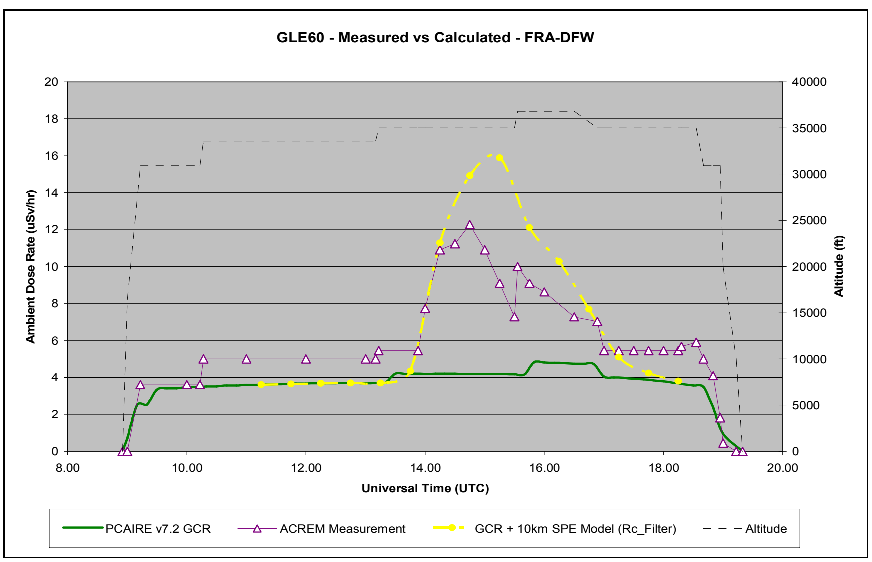

(b)

Figures 5 (a) Comparison of calculations and measurements of the ambient dose equivalent rates during GLE 60 for PRG-JFK flight and (b) FRA-DFW flight.

Another GLE where actual measurements were taken was GLE65. The measurements were provided by Beck *et al*, and the comparison between our model and the data can be seen in Figure 6. In general, there is good agreement between the model predictions and the measured ambient dose equivalent rates for both GCR and the enhanced rates due to SPEs.

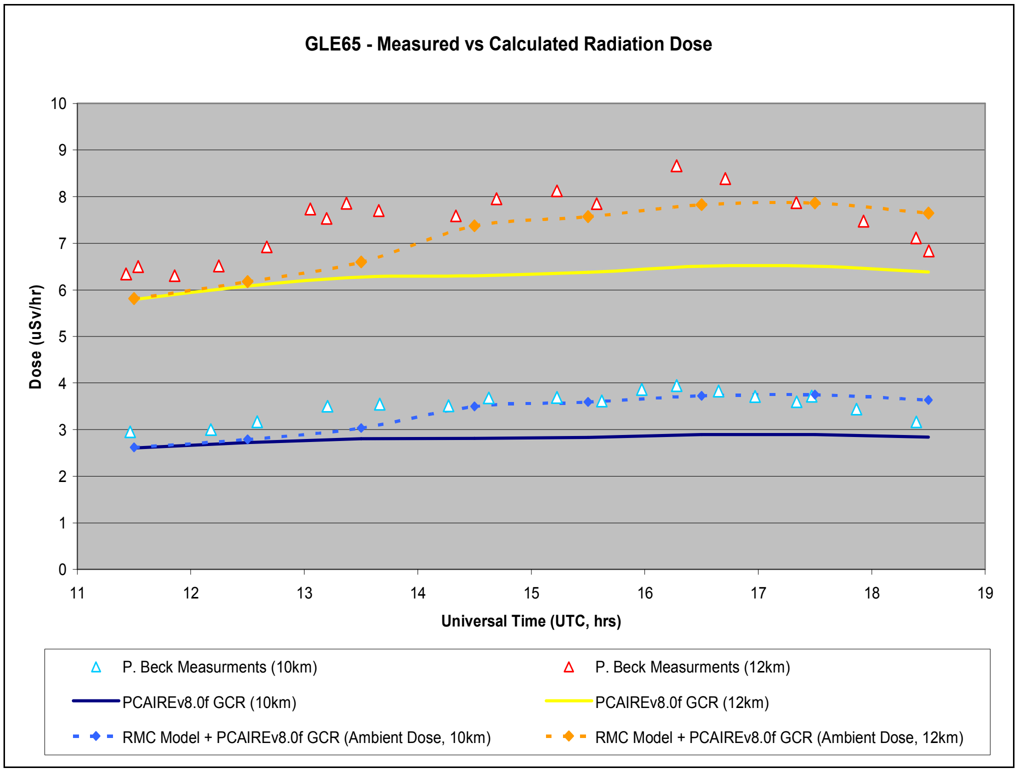

Figure 6 - Comparison of calculations and measurements of the ambient dose equivalent rates during GLE 65.

4. Summary and Conclusions

A transport code analysis using MCNPX was used to propagate an extrapolated particle spectrum based on GOES satellite measurements through the atmosphere to estimate aircrew radiation exposure due to solar flares. The calculation was benchmarked against actual flights measurements as well as neutron monitor data recorded on ground level. A computer code has been developed to implement the calculation with the possibility of including real-time monitoring in the near future.

5. References

[1] International Commission on Radiological Protection, *1990 Recommendations of the International Commission on Radiological Protection*, ICRP Publication 60, Pergamon Press, Oxford (1991).

[2] Transport Canada, "Measures for Managing Exposure to Cosmic Radiation of Employees Working On Board Aircraft," Commercial and Business Aviation Advisory Circular No. 0183 (2001).

[3] W. Heinrich, S. Roesler and H. Schraube, "Physics of Cosmic Radiation Fields," *Radiation Protection Dosimetry*, **86**(4), 253-258 (1999).

[4] B.J. Lewis, M. Desormeaux, A.R. Green, L.G. I. Bennett, A. Butler, M. McCall and J.C. Saez Vergara, "Assessment of Aircrew Radiation Exposure by Further Measurements and Model Development," *Radiation Protection Dosimetry,* **111**(2), 151-171 (2004).

[5] International Organization for Standardization, "Probabilistic model for particle fluences and peak fluxes of solar energetic particles," ISO TS 15391, October 2004.

[6] M. Takada, B.J. Lewis, M. Boudreau, H. Al Anid, and L.G.I Bennet, "Modeling of Aircrew Radiation Exposure from Galactic Cosmic Rays and Solar Particle Events", *Radiation Protection Dosimetry*, DOI: 10.1093/RPD/NCM214 (2007)

[7] J.M. Clem, G. De Angelis, P. Goldhagen and J.W. Wilson, *Radiation Protection Dosimetry*, 110(1/4), 423 (2004).

[8] M.S. Gordon, P. Goldhagen, K.P. Rodbell, T.H. Zabel, H.H.K. Tang, J.M. Clem and P. Bailey, *IEEE Transactions on Nuclear Science*, 51(6), 3427 (2004).

[9] P. Goldhagen, J.M. Clem, and J.W. Wilson, *Advances in Space Research*, 32(1), 35 (2003).

Table 1: Energy channels for Protons, Alphas and Electrons for the GOES-11 Satellite (EPS and HEPAD)

Particle Type	Channel number	Energy range (MeV)	Detector Assembly	Particle Rigidity (MV)
Proton	P1	0.8 - 4	Telescope	
	P2	4 - 9	Telescope	
	P3	9 - 15	Telescope	168 – 130
	P4	15 - 40	Dome	277 – 168
	P5	40 - 80	Dome	396 – 277
	P6	80 - 165	Dome	580 – 396
	P7	165 - 500	Dome	1090 – 580
	P8	350 - 420	HEPAD	982 – 883
	P9	420 - 510	HEPAD	1103 –982
	P10	510 - 700	HEPAD	1343 – 1103
	P11	≥700	HEPAD	
Alpha	A1	4 – 10	Telescope	
	A2	10 – 21	Telescope	
	A3	21 – 60	Telescope	
	A4	60 – 150	Dome	
	A5	150 – 250	Dome	
	A6	300 – 500	Dome	
	A7	2560 – 3400	HEPAD	
	A8	≥3400	HEPAD	
Electron	E1	≥0.6	Dome	
	E2	≥2.0	Dome	
	E3	≥4.0	Dome	

Table 2: Details of Ground-Based Neutron Monitors around the World

Station	Latitude (deg)	Longitude (deg)	Altitude (m)	Air Depth (g cm^{-2})	Detector Type	Vertical Cut-off Rigidity (GV)
Alma-ata	43.25	76.92	3340	675	18NM64	6.61
Apatity	67.55	33.33	177	1000	18NM64	0.57
Athens	37.98	23.78	260	980	6NM64	8.53
Baksan	43.28	42.69	1700	820	6NM64	5.6
Barensburg	78.12	14.42	0	1000	6NM64	0.05
Calgary	51.08	-114.13	1128	883	12NM64	1.08
Cape Shmidt	68.55	180.32	0	1016	12NM64	0.45
Climax	39.37	-106.18	3400	672	IGY	2.99
Erevan	40.5	44.17	3250	700	18NM64	7.58
Fort-Smith	60	-112	0	1013.3	18NM64	0
Haleaka	20.72	-156.27	3052	830	18NM64	13.3
Herman	-34.42	19.23	26	1035	12NM64	4.58
Inuvik	68.35	-133.72	21	1033.3	18NM64	0.17
Irkustk	52.47	104.03	435	984	18NM64	3.64
Jungraujoch	46.55	7.98	3475	655.7	3NM64	4.54
Kerguelen	-49.35	70.27	33	1019.7	IGY	1.14
Kiel	54.3	10.1	54	1026.5	18NM64	2.36
Larc	-62.2	-58.96	40	999.3	6NM64	3
Lomnicky	49.2	20.22	2634	761.7	IGY	3.98
McMurdo	-77.9	166.6	48	992.5	18NM64	0
Moscow	55.47	37.32	200	1019.7	24NM64	2.43
Mawson-Antractica	-67.6	62.88	0	1009.52	18NM64	0.22
Mexico	19.33	-99.2	2274	794.4	6NM64	9.53
Nain	56.6	-61.7	0	1033.3	18NM64	0
Norilsk	69.26	88.05	0	1024.8	18NM64	0.58
Novosibirsk	54.48	83	163	1014.6	24NM64	0.58
Newark	39.7	-75.7	50	1033.3	9NM64	2.87
Oulu	65.06	25.47	0	1019.7	9NM64	2.09
Peawanuck	55	-85	0	1033.3	18NM64	7
Rome	41.9	12.52	60	1028.9	17NM64	6.32
Sanae	-71.67	-2.85	856	897.4	6NM64	0.86
South Pole	-90	0	2820	693.4	3NM64	0.09
Tbilisi	41.43	44.48	510	984	18NM64	6.73
Terre Adelie	-66.67	140.02	45	1006.5	9NM64	0.02
Thule-Greenland	76.6	-68.8	260	1025.1	9NM64	0
Tsumeb	-19.2	17.58	1240	897.4	18NM64	9.21
Tixie	71.36	128.54	0	1019.7	18NM64	0.48
Yakutsk	62.01	129.43	105	1019.7	18NM64	1.65